The pacemaker of snake heart is localized near the sinoatrial valve

Denis V. Abramochkin[a,b,c] , Vladislav S. Kuzmin[a,b,c], Vladimir Matchkov[d], Andrey A. Kamensky[a] and Tobias Wang[e]

[a]*Department of Human and Animal Physiology, Lomonosov Moscow State University, Leninskiye Gory, 1, 12, Moscow, Russia*

[b]*Laboratory of Cardiac Electrophysiology, National Medical Research Center for Cardiology, 3rd Cherepkovskaya, 15a, Moscow, Russia*

[c]*Department of Physiology, Pirogov Russian National Research Medical University, Ostrovityanova, 1a, Moscow, Russia*

[d] *MEMBRANES, Department of Biomedicine, Faculty of Health, University of Aarhus, Aarhus, Denmark*

[e] *Section of Zoophysiology, Institute of Biology, University of Aarhus, Aarhus, Denmark*

Corresponding author: Denis V. Abramochkin. Address: Russia, Moscow, Leninskije gory, 1, 12, Biological faculty of Lomonosov Moscow State University, Department of human and animal physiology; e-mail: abram340@mail.ru; phone: +7-916-603-05-02.

Keywords: heart, reptile, acetylcholine, ionic currents, action potential, pacemaker

Summary statement

Contraction of the python heart is initiated by pacemaker cells in the region between left leaflet of sinoatrial valve and posterior horn of the sinus venosus.

Abstract

To provide the first description of the exact location of primary pacemaker of the squamate heart, we used sharp microelectrode impalements and optical mapping of isolated sinus venosus preparations from Burmese pythons. We located the dominant pacemaker site at the base of the right leaflet of the sinoatrial valve (SAV), but latent pacemakers were also identified in a circular region around the SAV. Acetylcholine (10^{-5}M) or noradrenaline (10^{-}

© 2021. Published by The Company of Biologists Ltd.

Journal of Experimental Biology • Accepted manuscript

^{6}M) induced shifts of the leading pacemaker site to other points near the SAV. The ionic currents of most of the cardiomyocytes isolated enzymatically from the SAV region resembled those of typical working myocytes from the sinus venosus. However, seven cells lacked the background inward rectifier current (I_{K1}) and had a time-dependent hyperpolarization-induced inward current identified as the "funny" current (I_f). Therefore, region proximal to SAV demonstrates pacemaking activity and contains cells that resemble the electrophysiological properties of mammalian pacemaker myocytes.

Abbreviations

ACh	Acetylcholine
AP	action potential
APD50	AP duration at the level of 50% repolarization
HCN channels	Hyperpolarization-activated cyclic nucleotide–gated channels, often called "pacemaker" channels
NA	noradrenaline
SAV	sinoatrial valve
SDD	slow diastolic depolarization
SV	sinus venosus
I_f	funny current
I_{K1}	background inward rectifier potassium current
I_{Na}	fast sodium current

Introduction

Each contraction of the vertebrate heart is initiated by the spontaneous generation of electrical activity in specialised pacemaker tissue on the venous pole of the heart (reviewed by Burkhard et al., 2017). While both structure and function of the mammalian sinoatrial node are quite well understood, even the general principles of cardiac pacemaker location and function remain uncertain in other vertebrate classes. Such information is obviously essential to understand the evolution of cardiac rhythm generation and its regulation. Invertebrate hearts contain pacemaker cells that are scattered across the heart in a diffuse

Journal of Experimental Biology • Accepted manuscript

manner. For example, slow diastolic depolarization (SDD), the main electrophysiological marker of pacemaker activity, can be observed in any part of a lugworm heart (Abramochkin et al., 2010). In fishes, the cardiac pacemaker becomes a circular field located around the sinoatrial valve (Haverinen and Vornanen, 2007). Finally, the mammalian heart has a compact pacemaker structure- the sinoatrial node. Thus, the concentration of pacemaker cells in an anatomically distinct compact structure appears to be the general trend of pacemaker evolution. However, the particular steps of that evolution are still not well described.

The exact position of the pacemaker driving the cyclostome heart remains to be localised. In hagfishes, there is slow diastolic depolarization (SDD) in atrial myocardium (Arlock, 1975), and expression of HCN channels in the atrial tissue (Wilson et al., 2013). However, in lamprey both atrium and ventricle lack any features of pacemaker electrical activity (Haverinen et al., 2014). In elasmobranch fishes, nodal myocardial tissue appears across the entire sinus venosus (SV) (Ramos et al., 1996; Ramos, 2004), but electrophysiological evidence for pacemaker function in the SV has only been provided in sting-rays (Saito, 1969).

The SV and its myocardial layer are reduced in teleosts compared to elasmobranchs. In plaice (Santer and Cobb, 1972) and sculpin (Santer, 1985), the SV consists of myocardial bundles partly separated by connective tissue, and Saito (1969) provided electrophysiological evidence of pacemaker activity in SV of sea eel. However, in various Cyprinids, salmonids and Atlantic cod, the SV lacks myocardium and consists mainly of connective tissue (Yamauchi et al., 1973; Yamauchi & Burnstock, 1968; Haverinen & Vornanen, 2007; Lukyanov et al., 1983). In these teleosts, nodal tissue is concentrated in a ring-like structure surrounding the sinoatrial valve (Haverinen & Vornanen, 2007; Yamauchi, 1980; Yousaf et al., 2012). Consistent with these histological observations, electrical activity typical for primary pacemaker of the heart, with smooth transition from SDD to action potential (AP) upstroke was found in a circle region at the base of the leaflets of the sinoatrial valve (SAV) (Lukyanov et al., 1983, 1986; Haverinen & Vornanen, 2007).

Trautwein and Zink (1952) provided classic recordings of pacemaker electrical activity in the SV of frogs using sharp microelectrodes, and a similar location of pacemaker was later confirmed in the toad *Bufo marinus* (Bramich et al., 1990). Hutter and Trautwein (1956), however, realised that only a small region within SV works as the primary pacemaker (the place where excitation originates in normal conditions), while the rest is

Journal of Experimental Biology • Accepted manuscript

excited by conduction and acts as subsidiary pacemaker, which also has automaticity, but less pronounced than that of primary pacemaker, at least in normal conditions. Moreover, the exact position of primary pacemaker within SV can move (pacemaker shift) under autonomic influence (Hutter and Trautwein, 1956). In mammals, the dominant pacemaker site is located in an anatomically distinct compact sinoatrial node at the border of the right atrium and the right sinus horn or superior caval vein (Monfredi et al., 2010; Boyett et al., 2003).

The location and function of the cardiac pacemaker is not well-known in reptiles, and there is conspicuous lack of electrophysiological information. Early pioneering studies by Walter H. Gaskell pointed to the cardiac pacemaker being placed in the SV of turtles (e.g. Gaskell, 1883), which was supported by later electrophysiological studies (Hutter and Trautwein, 1956), but immunohistochemical studies indicate pacemaker tissue at the border between SV and right atrium in Burmese pythons and Anolis lizard (Jensen et al., 2017). This location was supported by recordings with surface electrodes and points to a retrograde electrical activation of the SV (Jensen et al., 2017, 2014). The present study aims to determine the exact location of leading pacemaker site in the heart of Burmese python using the conventional sharp microelectrode technique and optical mapping.

Materials and methods

Experimental animals

Burmese pythons (*Python bivittatus*; Kuhl, 1920) of either sex with a body mass of 220-350g were kept at Aarhus University for several months in individual containers with free access to water, a temperature range of 26-32°C, and a humidity of 80%. They were fed weekly and gained mass in captivity, but had been fasted for two to three weeks before the hearts were studied. The experiments were performed in accordance with the Danish Law for Animal Experimentation.

Action potential recordings in multicellular preparations

The animals were killed by a sharp blow to the head, and the heart was rapidly excised and rinsed in physiological solution containing (in mmol l^{-1}) 115 NaCl, 2.5 KCl, 1 $MgSO_4$, 1.2 NaH_2PO_4, 5 glucose, 5 pyruvate, 2.5 $CaCl_2$ and 25 $NaHCO_3$ and had a pH of 7.7-7.8 when equilibrated with 2 kPa CO_2 in O_2 at 25-30 °C. The preparation containing the SV, the

Journal of Experimental Biology • Accepted manuscript

sinoatrial junction and the proximal piece of right atrium was cut off and pinned on the bottom of the Sylgard-coated chamber (3 ml in volume), where it was superfused with a constant flow of physiological saline solution (6 ml/min) at 30°C. The SV with right horn and posterior horn was opened and the left horn was cut off. The microelectrodes were always impaled from the endocardial side of SV. All preparations exhibited spontaneous contractions with stable rhythm throughout the experiments.

The recording of electrical activity commenced when the preparation had stabilized in the Ringer solution for 40 min. Conventional sharp glass microelectrodes were used for intracellular recording of electrical activity in the myocardium of SV. The microelectrodes were filled with 3 M KCl (40–80 MΩ) and connected to a high input impedance amplifier (Model 3100, A-M Systems, Carlsborg, WA, USA); microelectrodes needed a resistance above 40 MΩ for stable impalements. The signal was digitized and recorded using the Powergraph 3.3 (DI-Soft, Moscow, Russia), and analysed using MiniAnalysis 3.0 software (Synaptosoft, Fort Lee, NJ, USA). If acetylcholine or noradrenaline were applied the stable impalements were maintained during whole period of drug action. AP duration at 50% of repolarization (APD50), resting membrane potential, AP amplitude, AP upstroke velocity (dV/dt_{max}) and beating rate of the preparations were determined during off-line analysis.

Patch clamp measurements of ionic currents in isolated myocytes from python heart

Electrophysiological experiments were conducted on enzymatically isolated myocytes from the region surrounding the sinoatrial valve. The isolation procedure resembled our earlier methods for fish hearts (Abramochkin and Vornanen, 2015), but high enzyme concentrations (1.5 mg/mL collagenase Type IA and 1 mg/mL Trypsin IV) were needed to digest the considerable amount of connective tissue. A stainless steel cannula was inserted via the right aorta into the ventricle and secured with a fine thread. The left aorta and pulmonary artery were ligated to avoid leak and ensure completely retrograde flow from the ventricle to the atria. Initially, the heart was perfused at room temperature with Ca^{2+}-free solution for 20 min, whereupon hydrolytic enzymes and fatty acid-free serum albumin (Sigma) were added for next 40 min. Then, the SAV was separated from the rest of SV, minced and incubated in a similar enzyme solution on a shaker at room temperature. After another 40 min, the solution was replaced with enzyme-free solution of the same composition, the tissue was triturated with Pasteur pipette to obtain isolated cells. Myocytes were stored at 5°C and studied on the same day. The Ca^{2+}-free solution

Journal of Experimental Biology • Accepted manuscript

contained (in mmol l^{-1}) 100 NaCl, 10 KCl, 1.2 KH_2PO_4, 4 $MgSO_4$, 50 taurine, 20 glucose and 10 HEPES at pH 6.9 (adjusted with NaOH at 20°C).

The whole-cell voltage clamp recording of I_{K1} and I_f was performed using an Axopatch 200B amplifier (Molecular Devices, San Jose, CA, USA). Myocytes were superfused at room temperature (23±0.5°C) with an external saline solution containing (in mmol l^{-1}): 150 NaCl, 5.4 KCl, 1.8 $CaCl_2$, 1.2 $MgCl_2$, 10 glucose, 10 HEPES; pH adjusted to 7.6 at 20°C with NaOH. E-4031 (5×10^{-6} M) was continuously present in external solution to block I_{Kr}. Patch pipettes of 1.5-2.5 MΩ resistance were pulled from borosilicate glass (Sutter Instruments, Novato, CA, USA) and filled with K^+-based electrode solution containing (in mmol l^{-1}): 140 KCl, 1 $MgCl_2$, 5 EGTA, 4 MgATP, 0.3 Na_2GTP and 10 HEPES with pH adjusted to 7.2 with KOH. Series resistance and capacitances of pipette and cell were routinely compensated. Current amplitudes were normalized to the capacitive cell size (pA/pF).

Optical mapping of SV preparations

The spread of excitation in the SAV region was visualised by optical mapping, di-4-ANEPPS-based technique in multicellular preparations of SV, which were dissected as described previously (Abramochkin et al., 2020). The optical mapping rig included a photodiodes array (PDA, WuTech H-469V, Gaithersburg, MD, USA) designed for high speed data acquisition (1.63 Kfps). Macroscopic projections of the cardiac tissue preparations were transferred to the PDA with aid of the optical system including adapters and Computar V5013 (CBC Group, Japan) camera lens (focal length 50 mm, aperture ratio 1:1.3) mounted in distance of 24 mm from tissue surface. The optical system allowed to project an area of 5 mm in diameter to a hexagonal array of 464 PDA photodiodes; each photodiode covered the surface of 0.23 mm in diameter approximately. The view-field was projected also to the monitoring CCD camera (NexImage, Celestron, USA) used to match the mapping area and sites in the tissue preparations. An excitation light was emitted by LED (520±40 nm) arrays surrounding the experimental chamber with mapped preparation. A long-pass emission filter (λ>650 nm) was positioned in front of the camera lens.

After dissection, SV preparations were placed into experimental chamber and superfused with a constant flow of 30°C physiological saline solution (6 ml/min) of the same composition as used for microelectrode experiments. Voltage-sensitive dye di-4-ANEPPS (5 mg/mL, dissolved in DMSO) was added to physiological solution (final concentration 5×10^{-5} M) for 30 min staining of preparation. Then preparations were

Journal of Experimental Biology • Accepted manuscript

equilibrated for 20 min prior to mapping procedure. To suppress mechanical artefacts, the electromechanical uncoupler blebbistatin (5×10^{-5} M) was added to the perfusion solution.

Optical mapping data analysis

In all experiments fluorescent signals (optical APs) were recorded continuously for 5 s with 0.614 ms frame intervals, digitized using a data acquisition system (CardioPDA-III; RedShirtImaging, Decatur, GA, USA) and analyzed using Cardioplex (v.8.2.1, RedShirtImaging) software. Resting fluorescence was determined before each recording. Signals were processed via Savitsky-Golay filter using custom algorithm to remove noise and were normalized to the resting fluorescence level. Also, minimal high-pass filter was applied to remove slow photodiode-derived basal drift. The maximum upstroke derivative (dF/dtmax) for each optical AP was calculated to determine the activation times in the mapped areas. Isochronic activation maps were constructed from activation times using an in-house developed software. The area of an initial activation was defined as area covered by depolarization in first 2 ms after the start of excitation. The localization of the primary activation sites was defined as a center of the 2 ms activated area.

Drugs

E-4031 was purchased from Tocris (Bristol, UK). Collagenase type IA, trypsin, noradrenaline (NA), blebbistatin, $BaCl_2$ and acetylcholine chloride (ACh) were purchased from Sigma (St. Louis, MO, USA), and Di-4-ANNEPS from Thermo Fisher Scientific.

Statistics

All data are expressed as mean±s.e.m. Effects of ACh and NA on AP waveform and optical mapping parameters were evaluated using paired t-test. A p-value of 0.05 was regarded as the limit of statistical significance.

Results and Discussion

Search for pacemaker electrical activity in SV using microelectrode technique

The isolated SV preparations from pythons exhibited stable, spontaneous and rhythmic contractions (40.2±2.3 min^{-1}; n=13) with stable AP waveform for several hours when superfused with oxygenated physiological solution (see Abramochkin et al., 2020).

Journal of Experimental Biology • Accepted manuscript

In the major part of SV (whole posterior horn, right horn, see Fig.1a), we only observed electrical activities with features of the working myocardium; i.e. a stable negative resting potential of -81.3±1.5 mV, large AP amplitude of 109.2±3.1 mV and fast AP upstroke with dV/dt_{max} of 56±3.2 V/s (n=7). The APD50 was 350.2±5.9 ms. In this type of SV myocardium, ACh (10^{-6}M) greatly shortened APD50 by 91.5±3.1% of the control value and caused a small, but significant decrease in AP amplitude by 17.9±2.1% without significant changes in resting membrane potential (n=6). However, the rate of spontaneous APs only decreased by 6.4±1.8% of control (n=6). Higher ACh concentration (10^{-5}M) induced almost similar effects (Fig. 1b) with exception of slower rhythm by as much as a 21.4±4.2% reduction (n=5). NA (10^{-6}M) transiently prolonged the APs (Fig. 1c). Within 1 min of NA application, APD50 was 10.6±2.3% longer than before NA (n=5), but this effect subsided within 7 min, although AP amplitude tended to increase. NA accelerated the spontaneous rhythm 1 min after drug application, and reached 133.2±7.4% after 7 min.

We successfully impaled six preparations with microelectrodes to identify the specific location for pacemaker activity, *i.e.* SDD and APs with slow upstroke. In all six preparations, we could record electrical activity with SDD in a circular region around the SAV, but not further than 1.5 mm from the SAV (Fig. 1a). However, in SAV leaflets, which consist of myocardial tissue, we found no evidence for SDD. Furthermore, the AP waveform was the same as in posterior or right horn of SV. Electrical activity in the region around SAV was very heterogeneous in terms of SDD velocity, AP amplitude and upstroke velocity, as well as AP duration (Fig. 1a). Therefore, for further investigation we selected the pattern of electrical activity characterized by smooth transition from SDD to upstroke of AP (primary pacemaker at Fig. 1a). This pattern was first hypothesized by Hutter and Trautwein (1956) to be characteristic for the primary (leading) pacemaker site and that assumption was confirmed in numerous mapping studies (Bleeker et al., 1980; Vinogradova et al., 1998; Abramochkin et al., 2009). Electrical activity in primary pacemaker sites of python SV was also characterized by low dV/dt_{max} of 1.42±0.13 V/s, low AP amplitude of 74.4±3.8 mV and very long APs with APD50 of 602.6±57.5 ms (n=6 for each parameter). The stable resting membrane potential was absent in these sites due to SDD, but the value of maximal diastolic potential was -63.7±4.2 mV (n=6). The velocity of SDD was 27.3±2.48 mV/s (n=6). In all 6 preparations the primary pacemaker sites were located near the basement of the left leaflet of SAV (Fig.1a)

Journal of Experimental Biology • Accepted manuscript

At the leading pacemaker site, ACh and NA caused principally different effects to those observed in the major ("working") part of SV. ACh (10^{-5}M) produced prominent hyperpolarization, a decrease in AP amplitude and slowed the SDD by 66.7±7.4% (n=5) of control SDD velocity; leading to slower rhythm generation (Fig. 1d). At the same time, no drastic AP shortening, like in working SV myocardium, was observed. NA (10^{-6}M) did not affect maximal diastolic potential and AP amplitude, but increased SDD velocity by 82.8±7.5% of control and accelerated the rhythm (Fig. 1e).

Thus, electrical activity at the base of the SAV left leaflet differed entirely from the working myocardium in the SV and responded differently to ACh and NA: neurotransmitters greatly affect the SDD slope, but changed AP waveform less than in the working myocardium. Since the microelectrodes only allow recordings of electrical activity at a single point of the preparation, we also used optical mapping to analyse the activation sequence to identify the position of leading pacemaker in the SV from pythons.

Activation sequence of the snake SV revealed by optical mapping

The optical mapping were performed on similar preparations as those studied with microelectrodes. The site of the earliest activation, i.e. the leading pacemaker site, was located 1.5-2 mm from the left leaflet of SAV (Fig. 2b). No specialized conduction pathways or conductive corridors were observed in surroundings of primary pacemaker sites under control conditions. However, from there the excitation spread with low anisotropy directed predominantly circumferentially to SAV border. A second, minor site of early activation could be found in the mapped region in two of the five preparations (see Fig. 2). The area of the primary activation zone covered 1.7±0.4 mm^2 (n=5) in control conditions, which is less than 5% of total SV square.

ACh (10^{-5}M) shifted leading pacemaker site towards the SAV (Fig.2c). At the same time, the region where leading pacemaker was located in normal conditions turned into zone of slow conduction (activation with >10 ms delay after leading site). Under action by 10^{-6}M NA, a number of sites located right near SAV left leaflet started to activate almost synchronously (Fig.2d), but the region of primary pacemaker activity in control conditions, lost its dominance, like under the cholinergic influence. Due to delocalized primary excitation and lack of zones with a slow conduction in the presence of NA the excitation

Journal of Experimental Biology • Accepted manuscript

covered 90% of the mapped area in SV in significantly shorter time in comparison to ACh application (13±4 and 22±4 ms, $p<0.05$).

Measurements of funny current in cells isolated from SAV region of python heart

At the last stage of our experiments, we confirmed the presence of pacemaker cardiac myocytes in the SAV region of pythons. The investigated cells could be easily be divided in two groups according to their electrophysiological properties. The first group of cells were usually elongated spindle-shaped (Fig. 3a) with a mean capacitance of 30.1±1.1 pF (n=48) and a clear inward rectifier I_{K1} current during the hyperpolarizing ramp protocol (Fig. 3c). Square-pulse hyperpolarization to potentials from -100 to -160 mV induced instantaneous inward current (Fig. 3e), which was attributed to inward component of I_{K1}. Note also the large peak inward current, I_{Na}, induced by return of membrane potential to holding level (-35 mV).

Cells of the second group were elongate or "short-spindle" shaped (Fig.3b) and much smaller (capacitance of 17.1±1.9 pF, n=7, $p<0.05$). They were very scarce, merely 13% of all myocytes studies. They lacked a distinct I_{K1} current (Fig. 3d), but hyperpolarization to potentials from -100 to -160 mV induced a time-dependent inward current (Fig. 3f), which was similar in size to I_{K1} recorded in first group of cells. No or tiny peak I_{Na} was observed after return to -35 mV (Fig. 3f). The time-dependent hyperpolarization-induced inward current could be abolished by 2 mM Cs^{2+} (Fig. 3f, inset). Its mean I-V curve was typical for "funny" current (I_f) recorded in mammalian sinoatrial node cells (Verkerk et al., 2007), although shifted left by 10-20 mV (Fig. 3g). Therefore, we assume that recorded current in the second type of cells is I_f.

It is likely that the first group of cells represents working myocytes of SV, while the second group consists of true pacemaker cells that express I_f current. However, given that the I_f current in the second cell types is negligible at potentials within the physiological limits, the physiological role of these cells remains uncertain.

In summary, both microelectrode and optical mapping data point to the region between left leaflet of SAV and posterior horn of SV as the position of leading pacemaker site in the python heart under normal conditions. However, all the circular zone around the SAV should be considered as subsidiary pacemaker region. Points within that circular zone can work as leading pacemaker sites under the influence of autonomic neurotransmitters as in mammalian hearts (Bleeker et al., 1980; Shibata et al., 2001; Abramochkin et al., 2009).

Journal of Experimental Biology • Accepted manuscript

Cells with specific electrophysiological properties similar to those of mammalian pacemaker cells may be isolated from the SAV region. These cells lack I_{K1} and I_{Na}, but have "funny" current.

Acknowledgements Authors are grateful to Elin Petersen for excellent technical assistance and Heidi Meldgaard for devoted animal care.

Conflict of interests The authors have no conflicts of interest**.**

Funding The study was supported by the Danish Research Council (Natur og Univers, Danmarks Frie Forskningsfond), the Russian Science Foundation (19-15-00163, only optical mapping experiments) and the Interdisciplinary Scientific and Educational School of Moscow University «Molecular Technologies of the Living Systems and Synthetic Biology».

References

Abramochkin, D.V and Vornanen, M. (2015). Seasonal acclimatization of the cardiac potassium currents (I_{K1} and I_{Kr}) in an arctic marine teleost, the navaga cod (*Eleginus navaga*). *J. Comp. Physiol. B* **185**, 883-890.

Abramochkin, D.V., Kuzmin, V.S., Sukhova, G.S. and Rosenshtraukh, L.V. (2009). Modulation of rabbit sinoatrial node activation sequence by acetylcholine and isoproterenol investigated with optical mapping technique. *Acta Physiol.* **196**, 385-394.

Abramochkin, D.V., Matchkov, V. and Wang, T. (2020). A characterization of the electrophysiological properties of the cardiomyocytes from ventricle, atrium and sinus venosus of the snake heart. *J. Comp. Physiol. B* **190**, 63-73.

Abramochkin, D.V., Tennova, N.V., Hirazova, E.E., Pizgareva, A.V., Kuzmin, V.S. and Sukhova, G.S. (2010). Bioelectrical activity in the heart of the lugworm *Arenicola marina*. *J. Comp. Physiol. B* **180**, 645-651.

Arlock, P. (1975). Electrical activity and mechanical response in the systemic heart and the portal vein heart of *Myxine glutinosa*. *Comp. Biochem. Physiol. A Comp. Physiol*. **51**, 521-522.

Journal of Experimental Biology • Accepted manuscript

Bleeker, W.K., Mackaay, A.J., Masson-Pevet, M., Bouman, L.N. and Becker, A.E. (1980). Functional and morphological organization of the rabbit sinus node. *Circ. Res.* **46**, 11-22.

Boyett, M.R., Dobrzynski, H., Lancaster, M.K., Jones, S.A., Honjo, H. and Kodama, I. (2003). Sophisticated architecture is required for the sinoatrial node to perform its normal pacemaker function. *J. Cardiovasc. Electrophysiol*. **14**, 104-106.

Bramich, N.J., Edwards, F.R. and Hirst, G.D.S. (1990). Sympathetic nerve stimulation and applied transmitters on the sinus venosus of the toad. *J. Physiol*. **429**, 349-375.

Burkhard, S., van Eif, V., Garric, L., Christoffels, V.M. and Bakkers, J. (2017). On the evolution of the cardiac pacemaker. *J. Cardiovasc. Dev. Dis.* **4**, 4.

Gaskell, W.H. (1883). On the innervation of the heart, with especial reference to the heart of the tortoise. *J. Physiol*. **4**, 43-230.

Haverinen, J. and Vornanen, M. (2007). Temperature acclimation modifies sinoatrial pacemaker mechanism of the rainbow trout heart. *Am. J. Physiol.* **292**, R1023-R1032.

Haverinen, J., Egginton, S. and Vornanen, M. (2014). Electrical excitation of the heart in a basal vertebrate, the European river lamprey (*Lampetra fluviatilis*). *Physiol. Biochem. Zool*. **87**, 817-828.

Hutter, O.F. and Trautwein, W. (1956). Vagal and sympathetic effects on the pacemaker fibers in the sinus venosus of the heart. *J. Gen. Physiol*. **39**, 715-733.

Jensen, B., Boukens, B.J.D., Wang, T., Moorman, A.F.M. and Christoffels, V.M. (2014). Evolution of the SV from fish to humans. *J. Cardiovasc. Dev. Dis.* **1**, 14-28.

Jensen, B., Moorman, A.F. and Wang, T. (2014). Structure and function of the hearts of lizards and snakes. *Biol. Rev.* **89**, 302-336.

Jensen, B., Vesterskov, S., Boukens, B.J., Nielsen, J.M., Moorman, A.F.M., Christoffels, V.M. and Wang, T. (2017). Morpho-functional characterization of the systemic venous pole of the reptile heart. *Sci. Rep*. **7**, 6644.

Lukyanov, A.N., Sukhova, G.S. and Chudakov, L.I. (1986). Mechanism of variation in the general rhythm of the heart pacemaker in the cod Gadus morhua in response to vagal stimulation. *J. Evol. Biochem. Physiol.* **22**, 25-30.

Journal of Experimental Biology • Accepted manuscript

Lukyanov, A.N., Sukhova, G.S. and Udel'nov, M.G. (1983). Localization structural and functional organization of cardiac pacemaker in the cod Gadus morhua. *Zh. Evol. Biokhim. Fiziol*. **19**, 231-236.

Monfredi, O., Dobrzynski, H., Mondal, T., Boyett, M.R. and Morris, G.M. (2010). The anatomy and physiology of the sinoatrial node – a contemporary review. *Pacing Clin. Electrophysiol*. **33**, 1392-1406.

Ramos, C., Munoz-Chapuli, R. and Navarro, P. (1996). Ultrastructural study of the myocardium of the sinus venosus and sinoatrial valve in the dogfish (Scyliorhinus canicula). *J. Zool. Lond*. **238**, 611-621.

Ramos., C. (2004). The structure and ultrastructure of the sinus venosus in the mature dogfish (*Scyliorhinus canicula*): the endocardium, the epicardium and the subepicardial space. *Tissue and Cell* **36**, 399-407.

Saito, T. (1969). Electrophysiological studies on the pacemaker of several fish hearts. *Zool. Mag.* **78**, 291-296.

Santer, R.M. (1985). Morphology and innervation of the fish heart. *Adv. Anat. Embryol. Cell. Biol.* **89**, 1-102.

Santer, R.M. and Cobb, J.L. (1972). The fine structure of the heart of the teleost, *Pleuronectes platessa* L. *Z. Zellforsch Mikrosk. Anat.* **131**, 1-14.

Shibata, N., Inada, S., Mitsui, K., Honjo, H., Yamamoto, M., Niwa, R., Boyett, M.R. and Kodama, I. (2001). Pacemaker shift in the rabbit sinoatrial node in response to vagal nerve stimulation. *Exp. Physiol.* **86**, 177-184.

Trautwein, W. and Zink, K. (1952). Uber Membran- und Aktionspotentiale einzelner Myokardfasern des Kalt- und Warmbluterherzens. *Pflugers Arch*. **256**, 68-84.

Verkerk, A.O., Wilders, R., van Borren, M.M., Peters, R.J., Broekhuis, E., Lam, K., Coronel., R., de Bakker, J.M. and Tan, H.L. (2007). Pacemaker current (I_f) in the human sinoatrial node. *Eur. Heart J.* **28**, 2472-2478.

Vinogradova, T.M., Fedorov, V.V., Yuzyuk, T.N., Zaitsev, A.V. and Rosenshtraukh, L.V. (1998). Local cholinergic suppression of pacemaker activity in the rabbit sinoatrial node. *J. Cardiovasc. Pharmacol.* **32**, 413-424.

Journal of Experimental Biology • Accepted manuscript

Wilson, C.M., Stecyk, J.A., Couturier, C.S., Nilsson, G.E. and Farrell, A.P. (2013). Phylogeny and effects of anoxia on hyperpolarization-activated cyclic nucleotide-gated channel gene expression in the heart of a primitive chordate, the Pacific hagfish (*Eptatretus stoutii). J. Exp. Biol*. **216**, 4462-4472.

Yamauchi, A. (1980). Fine structure of the fish heart. In *Heart and heart-like organs* (ed. G. H. Bourne), pp. 119-148. New York: Academic Press.

Yamauchi, A. and Burnstock, G. (1968). An electron microscopic study on the innervation of the trout heart. *J. Comp. Neur.* **132**, 567-588.

Yamauchi, A., Fujimaki, Y. and Yokota, R. (1973). Fine structural studies of the sino-auricular nodal tissue in the heart of a teleost fish, *Misgurnus*, with particular reference to the cardiac internuncial cell. *Am. J. Anat.* **138**, 407-430.

Yousaf, M.N., Amin, A.B., Koppang, E.O., Vuolteenaho, O., Powell, M.D. (2012). Localization of natriuretic peptides in the cardiac pacemaker of Atlantic salmon (*Salmo salar* L.). *Acta Histochem.* **114**, 819-826.

Journal of Experimental Biology • Accepted manuscript

Figures

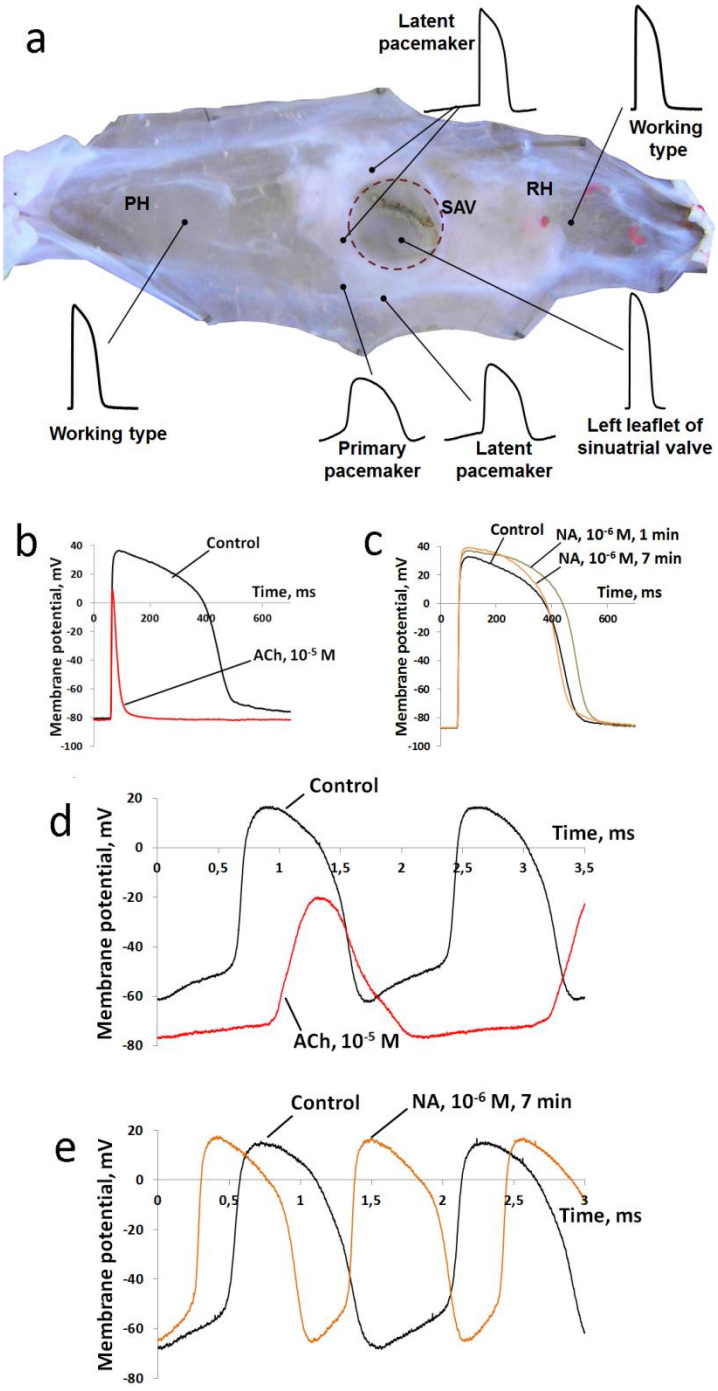

Figure 1 Electrical activity of pacemaker type and working myocardium type in the SV of Burmese python. **a** – photograph of typical preparation of SV showing the most usual sites where depicted types of electrical activity could be recorded. RH – right horn, PH – posterior horn, SAV – sinoatrial valve. **b,c** – original recordings of APs recorded from working myocardium of representative SV preparations in control conditions and

Journal of Experimental Biology • Accepted manuscript

under the action of 10^{-5}M ACh (**b**, after 3 min of application) or 10^{-6}M noradrenaline (**c**, traces recorded after 1 and 7 min of drug application are shown). d, e - original recordings of electrical activity recorded from the site of primary pacemaker in representative SV preparations in control conditions and under the action of 10^{-5}M ACh (**d**, 3 min after application) or 10^{-6}M noradrenaline (**e**, 7 min after application).

Journal of Experimental Biology • Accepted manuscript

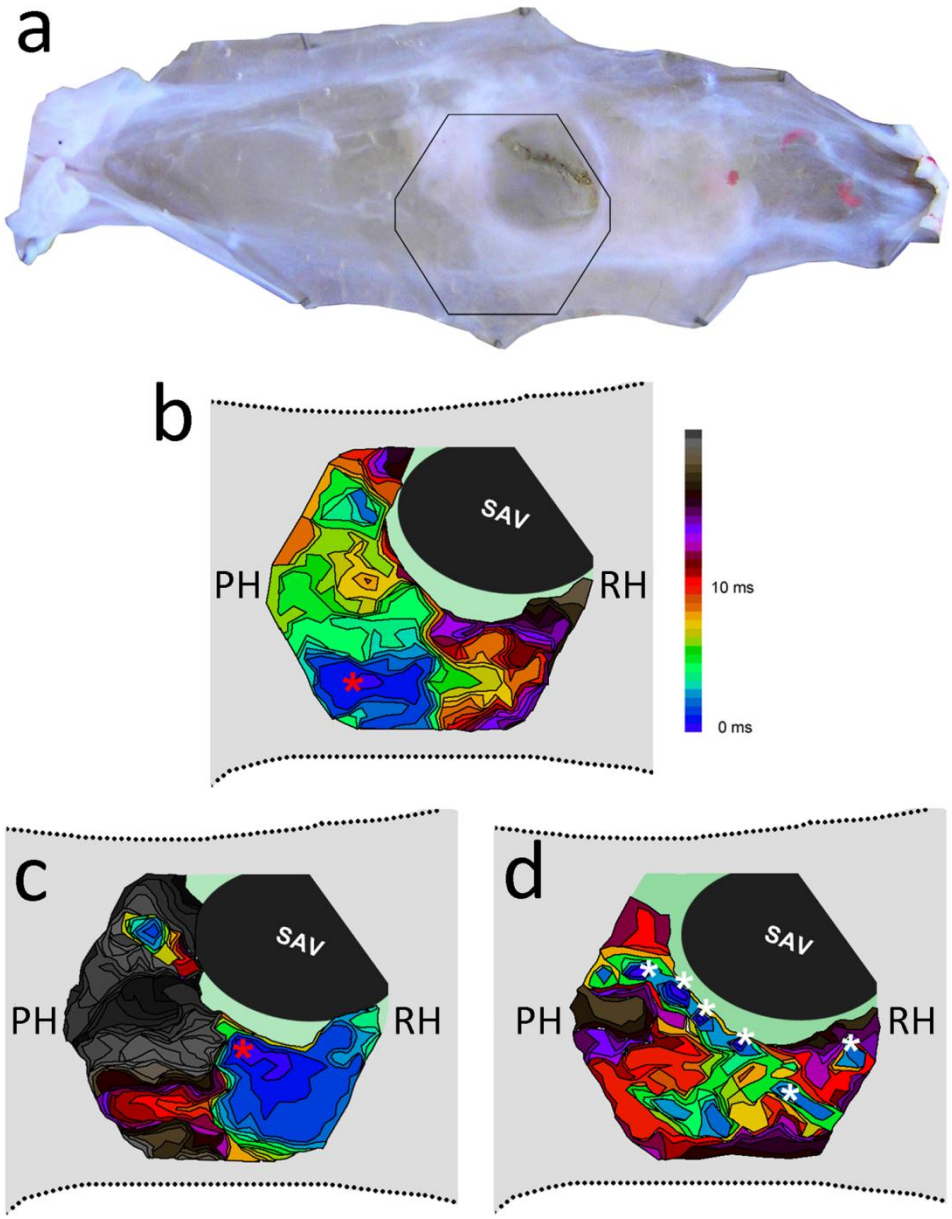

Figure 2 Activation sequence of python SV revealed by optical mapping. a - photograph of typical preparation of python SV showing the location of area investigated by optical mapping. b,c,d – isochronal map of SV fragment marked at panel a, in control conditions (b) and under the effect of 10^{-5}M ACh (c) or 10^{-6}M NA (d). All three maps were obtained from the same representative preparation. RH – right horn, PH – posterior horn, SAV – sinoatrial valve. Blue color indicates regions of the earliest excitation. Asterisks mark the particular points of earliest excitation.

Journal of Experimental Biology • Accepted manuscript

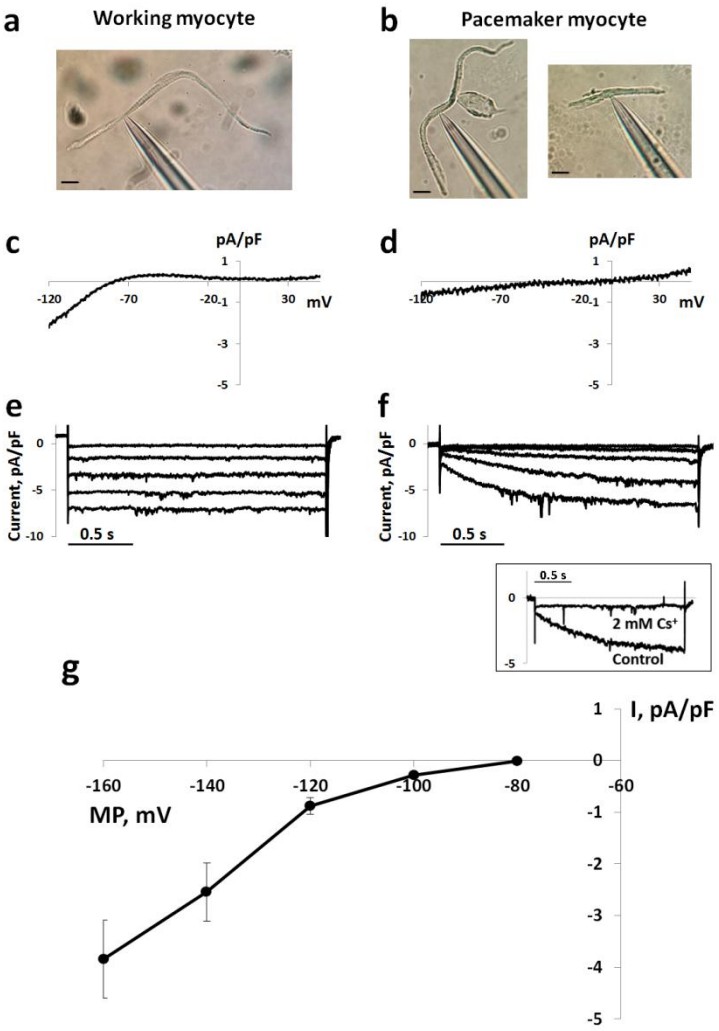

Figure 3 Distinguishing pacemaker and working cardiomyocytes isolated from python SAV region by their electrophysiological properties. **a,b** – photographs of myocytes isolated from python SV: a typical myocyte with "working" electrophysiological phenotype (**a**) and two myocytes with pacemaker electrophysiological phenotype (**b**). **c,d** – original I-V curves of the current elicited by hyperpolarizing ramp (from +60 to -120 mV) protocol in representative working (**c** – note distinctive I_{K1} inward rectifier) and pacemaker (**d** – no I_{K1}) myocytes. **e,f** – original traces of current elicited by square-pulse hyperpolarizing steps from holding potential of -35 mV to -80-160 mV in representative working (**e** – no time-dependent current) and pacemaker (**f** – note time-dependent inward current induced by hyperpolarization) myocytes. The block of time-dependent current at -140 mV by 2 mM Cs^+ is shown in the inset. **g** – mean±s.e.m. I-V curve of peak hyperpolarization-activated current recorded in pacemaker myocytes isolated from python SAV region (n=7 cells from 5 snakes).

Journal of Experimental Biology • Accepted manuscript